Hindawi
Advances in Civil Engineering
Volume 2019, Article ID 1348767, 18 pages
https://doi.org/10.1155/2019/1348767

Research Article

Probabilistic Analysis of Tunnel Liner Performance Using Random Field Theory

Xin Yu,[1,2] **Jinguo Cheng**,[2] **Chunhui Cao**,[1,2] **Erqiang Li**,[1,2] **and Jili Feng**[1,2]

[1]*State Key Laboratory for Deep Geomechanics and Underground Engineering, China University of Mining and Technology, Beijing 100083, China*
[2]*School of Mechanics and Civil Engineering, China University of Mining and Technology, Beijing 100083, China*

Correspondence should be addressed to Xin Yu; xinyu@student.cumtb.edu.cn

Received 8 July 2019; Accepted 1 August 2019; Published 21 August 2019

Academic Editor: Roberto Nascimbene

Tunnel liner is conventionally designed according to the deterministic design methods. However, the loads transmitted from the surrounding ground to the liner are very uncertain. In other words, the tunnel liner is subjected to nonuniform loading conditions which may affect its performance. This is mainly due to the inherent randomness and spatial variability of ground properties. In addition, since borehole drillings are usually carried out before tunnel excavation, the measured borehole data should be considered and reflected in the tunnel liner design practice, especially when it comes to the reliability-based design using the conditional random field theory. This paper presents an investigation of the tunnel liner performance from the perspective of probabilistic analysis and reliability-based design, and a probabilistic procedure for evaluating the tunnel liner performance is fully described. The random behavior of ground properties is accounted for by the conditional random field theory, and the performance of tunnel liner is examined via finite-difference modeling in FLAC 3D. The evaluation procedure is performed within the Monte Carlo simulation framework. An illustrative hypothesized tunnel is introduced to demonstrate the application of the probabilistic evaluation procedure, and the effects of site characterization parameters and conditioning on the tunnel liner performance are also inspected in a series of parametric studies. Before reaching conclusions, the reliability-based design of a real tunnel is performed with respect to the liner strengths and thickness, given target reliability levels, which provides some insights into a more reasonable and economical design of tunnel liner.

1. Introduction

In recent years, the investigation of tunnel liner has received more and more attention from researchers in geotechnical engineering, and an increasing number of relevant studies have been reported in the literature [1–10]. However, most of the studies listed above are devoted to either the deterministic analysis or design of tunnel liner or simple probabilistic analysis of tunnel liner stability with only consideration of the variability of ground properties.

For example, in the study presented by Carranza-Torres and Diederichs [1], the proposed methodology is deterministic for the mechanical analysis and design of composite tunnel liners consisting of shotcrete and steel sets. Moreover, in the investigation conducted by Langford and Diederichs [3], the modified point estimate method for the reliability-based analysis and design of tunnel liner considers only the variability of Hoek–Brown parameters. Furthermore, the simple probabilistic procedure initiated by Kroetz et al. [7] for analyzing the tunnel liner stability, with respect to the liner internal forces, can only account for the variability in the soil mass.

In geotechnical site investigation, one simple observation can be made that geotechnical materials close together in space may be much more similar in property than those separated widely. In addition, the spatial variability of geotechnical properties, such as soil properties, has long been recognized by geotechnical researchers (see, e.g., [11–16]) and has been incorporated in the random field theory [17] in the area of probabilistic analysis of slope

stability (e.g., [18–20]). As for the tunnel liner, a limited amount of documents have been reported with respect to the probabilistic analysis and design of tunnel liner with consideration of spatial variability of soil properties.

Another observation can also be made that when using random field theory to simulate the probabilistic nature of a particular geotechnical project, we often have investigation data available at that project site that should be considered and reflected in each simulation. In tunnel engineering, for example, an extensive borehole drilling investigation at the planned tunnel construction area is usually carried out before excavation occurs, which is used to identify the ground conditions as well as secure an efficient and low-risk construction. Therefore, it makes sense for any simulated geotechnical property random field to incorporate the core sampling data collected at the borehole locations in each and every simulation. In addition, the geotechnical properties should only be random between the borehole locations and become increasingly random as the distance from the borehole locations rises. In other words, the conditional random field theory [21, 22] should be applied in the simulation of geotechnical properties.

Although finite-element or finite-difference method, combined with probabilistic analysis tools, has been implemented in the geotechnical treatments (see, e.g., [23–31]), very few works can be found with respect to the combination of finite-element or finite-difference method with conditional random field theory in the area of tunnel liner stability analysis and design.

Thus, the current work is inspired by the limitations of previous studies. In this study, we focus on the probabilistic analysis of shallow tunnel liner performance using conditional random field theory as well as finite-difference modeling. This paper is organized as follows. In Section 2, the unconditional and conditional simulation of random fields is described. Then, the procedures for mapping the conditional property values onto the finite-difference model are developed and illustrated in Section 3. Next, the design failures of tunnel liner with respect to compression and tension effects are defined in Section 4. In Section 5, a probabilistic procedure for evaluating the tunnel liner performance is fully presented, followed by applying it into the parametric studies of the effects of site characterization parameters and conditioning on the tunnel liner performance in Section 6. In addition, the reliability-based design of a real tunnel is also conducted using that procedure in Section 7. Finally, a number of conclusions are drawn.

2. Simulation of Random Fields

2.1. Unconditional Random Field. A number of methods have been reported in the literature to simulate unconditional random field (URF). These include fast Fourier transform method [32], turning bands method [33], midpoint method [34], local average subdivision method [35], and Karhunen–Loève expansion method [36]. In this paper, the rationale of local average subdivision (LAS) is briefly illustrated.

The motivation for LAS comes from the need to properly account for the fact that most engineering measurements are actually local averages of the property in question [35]. Take the 2-dimensional random field as an example, the LAS method involves a recursive subdivision process in which a parent cell is divided into four equal-sized child cells. As the process continues, the field in question will become much finer discretized. Note that the global average remains constant throughout the subdivision process by requiring that the average of each four cells generated is equivalent to the parent cell value. A schematic diagram indicating the subdivision process is shown in Figure 1, in which the parent cells at the subdivision stage i are denoted $Z_l^i, l = 1, 2, 3, ...$, and the subdivided child cells are denoted Z_j^{i+1}, $j = 1, 2, 3, 4$. Interested readers are referred to references [35, 37] for a complete and thorough understanding of discretization of the random field by LAS.

2.2. Conditional Random Field. A random field conditioned upon some known values at corresponding locations in a field is called a conditional random field (CRF) [37]. Mathematically, the CRF can be expressed by

$$Z_c(x) = \left\{ Z(x) \,\middle|\, z(x_\alpha), \quad \alpha = 1, 2, \ldots, n_k \right\}, \tag{1}$$

where $Z_c(x)$ is the desired CRF at the spatial locations x; $Z(x)$ is the unconditional simulated random field; z_{x_α} is the collected values at the investigated locations $x_\alpha, \alpha = 1, 2, \ldots, n_k$, and n_k is the total number of investigated locations.

To generate CRF, the random field should be separated into two parts spatially: (1) $x_\alpha, \alpha = 1, 2, \ldots, n_k$, being those points at the measured locations, and at which the random field should take on the deterministic values $z(x_\alpha)$; (2) x_η, $\eta = 1, 2, \ldots, n - n_k$, being those points at the unmeasured locations, and at which possible random values should be simulated. That is, the subscripts α and η denote the known and unknown values, respectively, and n is the total number of points in the random field to be simulated.

There are a number of methods documented in the literature to simulate CRF. These include the Hoffman method [38–42], Bayesian method [43], and Kriging-based method [22, 44, 45]. Note that the algorithm, initially proposed by Hoffman and Ribak [38], for the construction of constrained (conditional) Gaussian random field is termed here Hoffman method. Although this algorithm is reformulated or redeveloped by different researchers later on for various applications, they are basically the same. In this study, the Hoffman method is adopted to simulate CRF because of its simplicity in application and efficiency in computation. The procedures for constructing CRF by the Hoffman method are as follows:

Step 1. Partition the random field into known x_α and unknown x_η points.

Step 2. Represent the standard Gaussian values $g(x_\alpha)$ as a function of known values $z(x_\alpha)$ by the inverse transformation function $F^{-1}(\cdot)$ (i.e., $g(x_\alpha) = F^{-1}[z(x_\alpha)]$).

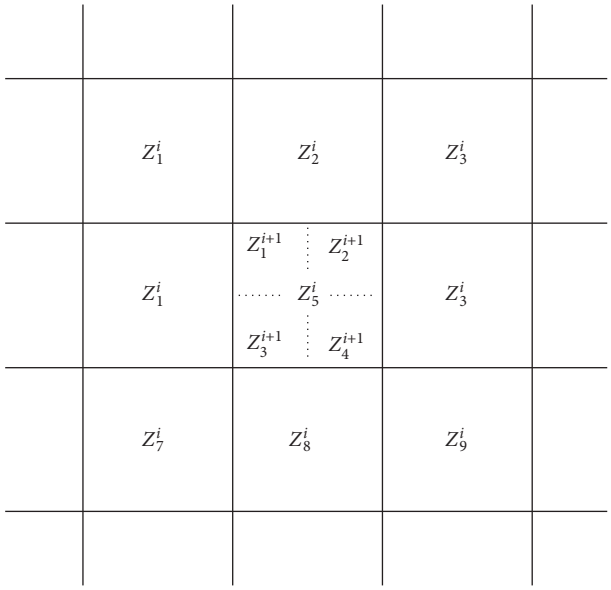

Figure 1: Schematic diagram of the subdivision process of LAS (after Ref. [37]).

Step 3. Simulate the unconditional standard Gaussian random field $G_u(x)$ at all points in the field by LAS, using zero mean, unit variance, autocorrelation structure $R = (R_{i,j})$, and cross-correlation structure ρ. Note that the unconditional random field is assumed to be stationary with mean and standard deviation unchanged throughout the domain.

Step 4. Form the covariance matrix $\mathbf{C}$ between the known points x_α using the equation below, and invert it to determine C^{-1}:

$$C = \left(R_{i,j}\right), \quad (i, j = 1, 2, \ldots, n_k). \tag{2}$$

Step 5. Similarly, form the covariance B between the unknown x_η and known x_α points using the following equation:

$$B = \left(R_{i,j}\right), \quad (i = 1, 2, \ldots n - n_k;\ j = 1, 2, \ldots, n_k). \tag{3}$$

Step 6. Generate the conditional standard Gaussian random field $G_c(x_\eta)$ by the following equation at the unknown points x_η:

$$G_c\left(x_\eta\right) = G_u\left(x_\eta\right) + BC^{-1}\left[g\left(x_\alpha\right) - G_u\left(x_\alpha\right)\right]. \tag{4}$$

Step 7. Transform the conditional Gaussian random field $G_c(x_\eta)$ into the target conditional random field $Z_c(x_\eta)$ by the following transformation:

$$Z_c\left(x_\eta\right) = F\left[G_c\left(x_\eta\right)\right]. \tag{5}$$

Step 8. Insert the known values $z(x_\alpha)$ into the generated conditional random field $Z_c(x_\eta)$ to form the overall conditional random field $Z_c(x)$.

It is worth mentioning that the unconditional simulation and conditioning processes in the above 8-step procedure are concerned with the unconditional standard Gaussian random field $G_u(x)$ and inversely transformed standard Gaussian values $g(x_\alpha)$, respectively, rather than the desired original random field $Z_u(x)$ and actual values $z(x_\alpha)$ collected at the measured points.

3. Random Property Mapping

Since the finite-difference code FLAC 3D [46] is capable of dealing with complex geological conditions of geotechnical problems, especially in the area of tunnel-related geotechnical treatments (e.g., [47–49]), it is used in this study to model and analyze the performance of tunnel liner with soil properties mapped from the CRF.

The present study is confined to the 2-dimensional plane strain conditions, and the finite-difference analysis of tunnel liner is performed with respect to the shield-driven tunnel at the cross-section level. Suppose the finite-difference model concerned has dimensions of $l \times l$ and is discretized into a total number of N zones. Then, the conditional property field generated can be mapped onto the corresponding finite-difference zone in terms of the zone centroid coordinates. Note that the conditional property field has the same dimensions as the finite-difference model.

It is assumed that the unconditional property field, which is used in the generation of the CRF, is subdivided n times to obtain a resolution of $2^n \times 2^n$. Then, the smallest subdivided cell has dimensions of $(l/2^n) \times (l/2^n)$ and the conditional property field can be denoted by a matrix of the form $A = (a_{m,n})$, $(m, n = 1, 2, \ldots, 2^n)$, in which each matrix element $a_{m,n}$ corresponds to the unique cell specified by the pair of subscript indices (m, n). For example, $a_{1,1}$ represents the lower-left cell, as shown in Figure 2. Note that the element values for the cells at the borehole locations are kept constant in each and every realization of the CRF.

Because the finite-difference model is composed of N zones and each zone has a zone centroid specified by its coordinates (x_i, z_i), $i = 1, \ldots, N$, we can find out the corresponding property matrix element in terms of the following equations:

$$m = \text{ceil}\left[\frac{x_i}{(l/2^n)}\right], \tag{6}$$

$$n = \text{ceil}\left[\frac{z_i}{(l/2^n)}\right], \tag{7}$$

where m and n are the subscript indices used to identify the corresponding property value $a_{m,n}$; ceil is a function to round $x_i/(l/2^n)$ and $z_i/(l/2^n)$ to the nearest integers towards infinity.

Hence, the property mapping procedure can be briefly summarized as follows:

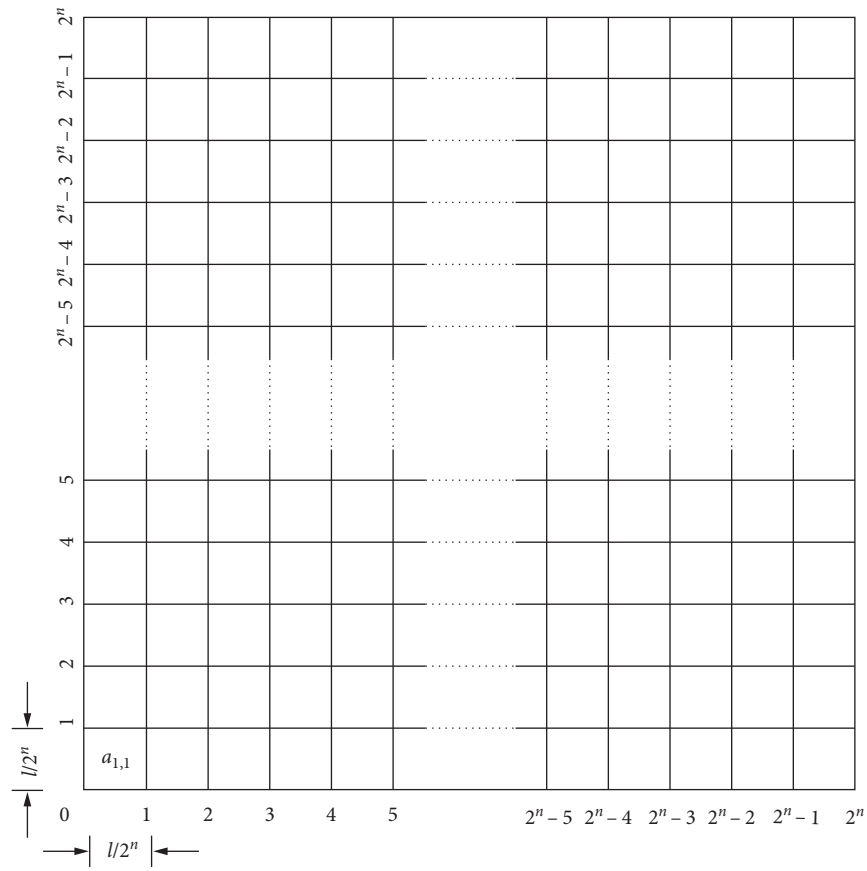

Figure 2: Random field cell values represented by matrix elements.

Step 1. Generate a realization of CRF and denote it as $A = (a_{m,n})$, $(m, n = 1, 2, \ldots, 2^n)$

Step 2. Obtain the finite-difference zone centroid coordinates (x_i, z_i), $i = 1, \ldots, N$ in FLAC 3D

Step 3. Positioning the zone centroid by calculating the pair of subscript indices (m, n) in terms of equations (6) and (7)

Step 4. Assign the random value $a_{m,n}$, which is specified by the pair of subscript indices (m, n) obtained in the above step, to the corresponding zone

Step 5. Repeat steps 3 to 4 until the finite-difference zones are all assigned

Note that a relatively higher resolution should be applied in the conditional property field generation process. Such that the smallest subdivided cell has dimensions no larger than the smallest finite-difference zone. This is done to ensure that the finite-difference mesh is sufficiently randomized, and thus, the effects of site characterization parameters and conditioning on the performance of tunnel liner can be fully taken account of.

4. Failure Modes of Tunnel Liner

The design of shallow tunnel liner involves two steps: (1) characterizing the relevant soil properties and (2) computing the axial stresses generated in the liner based on the characterized soil properties. The reliability of the tunnel liner depends on the relationship between the computed and true axial stresses in the liner. Disregarding the variability in tunnel liner and assuming that the liner resistance Q satisfies

$$Q = F_s \sigma_c^{\text{det}} = F_s \sigma_t^{\text{det}}, \tag{8}$$

where F_s is a factor of safety and σ_c^{det} and σ_t^{det} are the deterministic axial compressive and tensile stresses, respectively, computed based on the characterized soil properties.

Thus, the probability of failure of tunnel liner can be defined as the probability that actual compressive (tensile) stress, computed based on the randomized soil properties, is larger (less) than the factored liner resistance in terms of the design standards applied in the 2nd Avenue Subway Project in Manhattan, New York [50], and can be expressed as

$$\begin{aligned} p_{f,c} &= P\left[\sigma_c^{\text{act}} > F_s \sigma_c^{\text{det}}\right], \\ p_{f,t} &= P\left[\sigma_t^{\text{act}} < F_s \sigma_t^{\text{det}}\right], \end{aligned} \tag{9}$$

where $p_{f,c}$ and $p_{f,t}$ denote the compression and tension failure modes of tunnel liner, respectively; σ_c^{act} and σ_t^{act} are the actual compressive and tensile stresses, respectively, computed from the conditional random finite-difference modeling. It is assumed that the true (random) axial stresses can be closely approximated by the conditional random finite-difference modeling, which means that the realistic

estimates of true axial stresses can be obtained from each realization of the conditional random finite-difference analysis for a given set of random soil properties.

In this study, the simulated true axial stresses are normalized with respect to the computed deterministic axial stresses, as follows:

$$C_c = \frac{\sigma_c^{act}}{\sigma_c^{det}}, \qquad C_t = \frac{\sigma_t^{act}}{\sigma_t^{det}}, \tag{10}$$

where C_c and C_t are normalized compressive and tensile stress factors, respectively.

5. A Probabilistic Evaluation Procedure

Since the Monte Carlo simulation (MCS) has been widely applied to the reliability evaluation of geotechnical problems (see, e.g., [51–56]), in this paper it is included in the probabilistic evaluation framework, together with the finite-difference analysis, to estimate the performance of tunnel liner.

MCS is such a method that is often associated with estimating the probabilities of failure of complex systems to random inputs, especially when the analytical solutions are not available to the system. However, the problem with MCS is that if the probability of failure to be computed is rather small, as indicated by Fenton and Griffiths [37] that most civil engineering structures have a target failure probability p_f^t between $1/10^3$ and $1/10^6$, estimating such small failure probabilities typically requires a large number of simulation trials (i.e., at least $100/p_f^t$), which makes it very tedious; especially, when the simulation involves finite-element or finite-difference analysis, performing large numbers of simulations may be impractical.

In view of this, more efficient methods such as combining response surface method with subset simulation [22] and integrating MCS with distribution fitting [37] are developed. Since the latter method is much easier in implementation and the required reliability level of tunnel liner is around $1/10^4$ according to US Army Corps of Engineers [57], it is applied in this study to compute the probability of failure of tunnel liner.

Thus, the probabilistic procedures for evaluating the tunnel liner performance can be described as follows:

Step 1. Define the tunnel geometrical dimensions and discretize the domain into a set of finite-difference elements

Step 2. Determine the random soil properties and their statistics (i.e., the distribution type, autocorrelation function, correlation length, mean, coefficient of variation, and cross-correlation coefficient)

Step 3. Generate realizations of CRF by the Hoffman method described in Section 2.2 and map it onto the corresponding finite-difference element via the random property mapping procedure presented in Section 3

Step 4. Perform as many finite-difference analyses (e.g., 500 or more) as possible within the MCS loop to get a sufficient amount of desired responses (i.e., C_c and C_t)

Step 5. Construct the histogram for each of the obtained responses

Step 6. Fit an appropriate distribution to each of the constructed histograms

Step 7. Estimate the failure probability of tunnel liner under each failure mode with the corresponding distribution parameters fitted in Step 6

6. An Illustrative Example

In this section, a hypothesized simple tunnel is introduced to demonstrate the procedures for conducting a probabilistic analysis of the tunnel liner performance. Besides, the effects of site characterization parameters and conditioning on the tunnel liner performance are also investigated thoroughly in a series of parametric studies.

6.1. Problem Description. A shallow circular tunnel with radius $R = 1$ m, supported by concrete liner, is driven 30 m under the ground in the soil mass. The soil is assumed to be elastic, perfectly plastic with a Mohr–Coulomb failure criterion. The far-field boundaries are located at a distance of 10 tunnel radius from the tunnel axis. The two-dimensional finite-difference mesh is discretized into 3060 elements in total. The boundary conditions are such that in situ stresses of 600 kPa vertical and 300 kPa horizontal are installed at the top, left, and right sides. The bottom of the model is fully restrained.

Suppose that core drillings have been carried out at five different borehole locations separated by an equal interval of 5 m. Thus, the finite-difference elements within such borehole extent will be exposed and taken as core samples, as indicated in Figure 3 where borehole locations are represented by BH and exposed elements are in red. In addition, there are totally $n_k = 318$ core samples uncovered by the core drillings in the finite-difference mesh, which is to say that soil properties at such sample elements are completely determined.

It should be noted that the property values of the exposed sample elements at the borehole locations are randomly picked up from one of the realizations of unconditional simulation of the random field, and then these property values are kept invariant in each and every simulation of the conditional random field.

Since the cohesion and friction angle of soil are usually treated as lognormally distributed random variables in the literature (see, e.g., [58–60]), they are also randomized in the present study, while the rest Mohr–Coulomb parameters of soil and the tunnel liner properties are held constant for simplicity, as tabulated in Table 1.

The lognormally distributed cohesion and friction angle can be transformed from the standard normal distribution via the following equation:

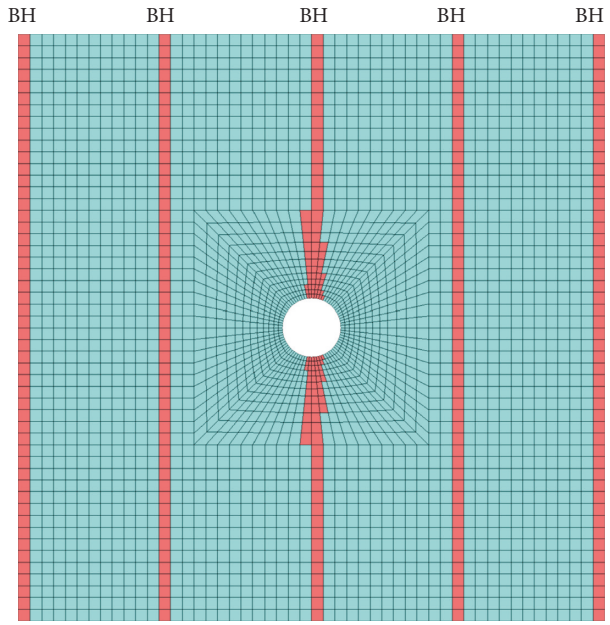

Figure 3: Supposed borehole locations and exposed elements.

Table 1: Deterministic input parameters for the hypothesized tunnel.

Category	Variable	Value
Soil	Young's modulus E_{soil} (MPa)	48
	Poisson's ratio ν_{soil}	0.34
	Dilation angle ψ (°)	0
Liner	Young's modulus E_{liner} (GPa)	25
	Poisson's ratio ν_{liner}	0.15
	Thickness t (mm)	50

$$y(x) = \exp\left[\mu_{\ln y} + \sigma_{\ln y} G_{\ln y}(x)\right], \tag{11}$$

where x is the spatial position of the desired variable y; the parameters $\mu_{\ln y}$ and $\sigma_{\ln y}$ are obtained from the variable mean μ_y and standard deviation σ_y using the following transformations:

$$\sigma^2_{\ln y} = \ln\left[1 + \left(\frac{\sigma_y}{\mu_y}\right)^2\right],$$
$$\mu_{\ln y} = \ln\left(\mu_y\right) - \frac{1}{2}\sigma^2_{\ln y}. \tag{12}$$

The autocorrelation function between cohesion and friction angle is assumed to be exponential in the form of

$$R_{i,j} = \exp\left(-\frac{2|x_i - x_j|}{\lambda_h} - \frac{2|z_i - z_j|}{\lambda_v}\right), \quad \left(i, j = 1, 2, \ldots, 2^8\right), \tag{13}$$

where $R_{i,j}$ is the spatial correlation between the ith and jth subdivided cells in the two-dimensional random field; note that the random field is subdivided 8 times to obtain a resolution of $2^8 \times 2^8$; λ_h and λ_v are the horizontal and vertical correlation lengths, respectively.

Since it is unlikely in practice to obtain a complete cross-correlation structure between cohesion and friction angle, a set of cross-correlation coefficients ranging from $\rho = -0.7$ to $\rho = 0.7$, as listed in Table 2, are assumed in the parametric studies that follow.

In order to make this study dimensionless, the coefficient of variation that is assumed to be the same for both cohesion and friction angle is used to represent soil property variability:

$$\text{cov} = \frac{\sigma_c}{\mu_c} = \frac{\sigma_\phi}{\mu_\phi}, \tag{14}$$

where σ_c, σ_ϕ and μ_c, μ_ϕ are the standard deviations and means of cohesion and friction angle, respectively. In addition, the horizontal and vertical correlation lengths are normalized with respect to the tunnel radius R, respectively, as follows:

$$\begin{cases} \theta_h = \dfrac{\lambda_h}{R}, \\ \theta_v = \dfrac{\lambda_v}{R}, \end{cases} \tag{15}$$

where θ_h and θ_v are the normalized horizontal and vertical correlation lengths, respectively.

In the parametric studies, the effects of site characterization parameters, including the coefficient of variation, horizontal (vertical) correlation length, and cross-correlation coefficient, on the probability of failure of tunnel liner are investigated. The mean cohesion ($\mu_c = 12380$ Pa) and mean friction angle ($\mu_\phi = 30°$) are held constant together with the rest soil and tunnel liner properties listed in Table 1, while the coefficient of variation, horizontal (vertical) correlation length, and cross-correlation coefficient are varied systematically according to Table 2. Notice that the site characterization parameters for both cohesion and friction angle are assumed to be the same in this study and changed simultaneously.

In order to maintain accuracy and run-time efficiency, an investigation of the sensitivity of mean strength factor (i.e., m_{C_c} and m_{C_t}) to the number of MCS trials is conducted. As can be seen from Figure 4, the mean strength factors all begin to converge after 5000 MCS trials or so. Thus, the MCS trials are determined to be 5000 in the parametric studies, which is believed to give accurate and reproducible results.

For each set of the 5000 computed strength factors (i.e., C_c^{CRF}, C_t^{CRF}, C_c^{URF}, and C_t^{URF}), a relative frequency histogram is plotted, followed by fitting an appropriate distribution to that histogram, as indicated in Figure 5. Note that the strength factors are normalized with the deterministic compressive and tensile strengths of $\sigma_c^{det} = 9.7$ MPa and $\sigma_t^{det} = -0.46$ MPa, respectively.

6.2. Effect of the Coefficient of Variation. Figures 6(a) and 6(b) show the effects of the coefficient of variation on the probability of compression and tension failures of tunnel liner, respectively, with consideration of both unconditional and conditional random fields. It can be seen that the coefficient of

Table 2: Parameters used in the parametric studies.

Parametric study	Site characterization parameter			
	cov	θ_h	θ_v	ρ
Effect of the coefficient of variation	0.1, 0.2, 0.3, 0.4, 0.5, 0.6, 0.7	20	5	−0.5
Effect of the horizontal correlation length	0.2	10, 20, 30, 40, 50, 60, 70	5	−0.5
Effect of the vertical correlation length	0.2	20	1, 2, 3, 4, 5, 6, 7	−0.5
Effect of the cross-correlation coefficient	0.2	20	5	−0.7, −0.5, −0.3, 0, 0.3, 0.5, 0.7

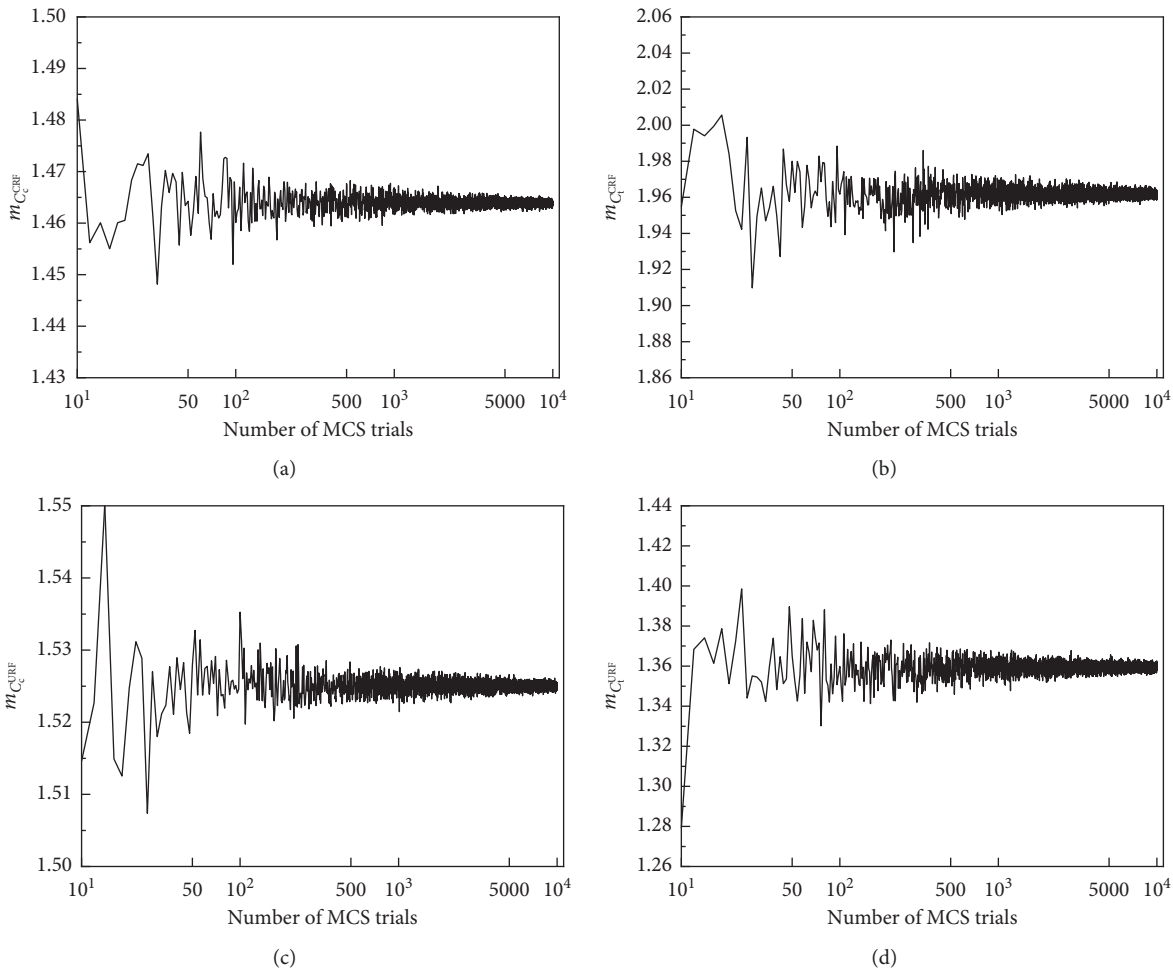

Figure 4: The sensitivity of mean strength factors to the number of MCS trials: (a) $m_{C_c^{CRF}}$, (b) $m_{C_t^{CRF}}$, (c) $m_{C_c^{URF}}$, and (d) $m_{C_t^{URF}}$.

variation can significantly affect the probability of failure. As anticipated, the probability of failure increases as the soil becomes increasingly variable. However, the rate of change of probability is small at low values of coefficient of variation, and then the failure probability goes up dramatically for moderately high coefficients of variation. As it continues to increase, the failure probability rises at a slower rate. It is also interesting to note that the probabilities based on the URF are always obviously greater than those based on the CRF, as shown in Figure 6(a). However, quite the opposite is observed in Figure 6(b) where the failure probabilities based on the URF are clearly lower than those based on the CRF.

6.3. Effect of the Horizontal Correlation Length. As can be seen from Figure 7(a), the horizontal correlation length has a minor effect on the probability of compression failure of tunnel liner under both unconditional and conditional random fields, and the failure probabilities based on the CRF are significantly lower than those based on the URF. However, quite the opposite is observed in Figure 7(b) where the effect of conditioning significantly increases the probability of tension failure. In addition, the failure probability based on the CRF gradually decreases as the horizontal correlation length increases, while the probability of tension failure based on the URF is almost unchanged as the horizontal correlation length varies, as shown in Figure 7(b).

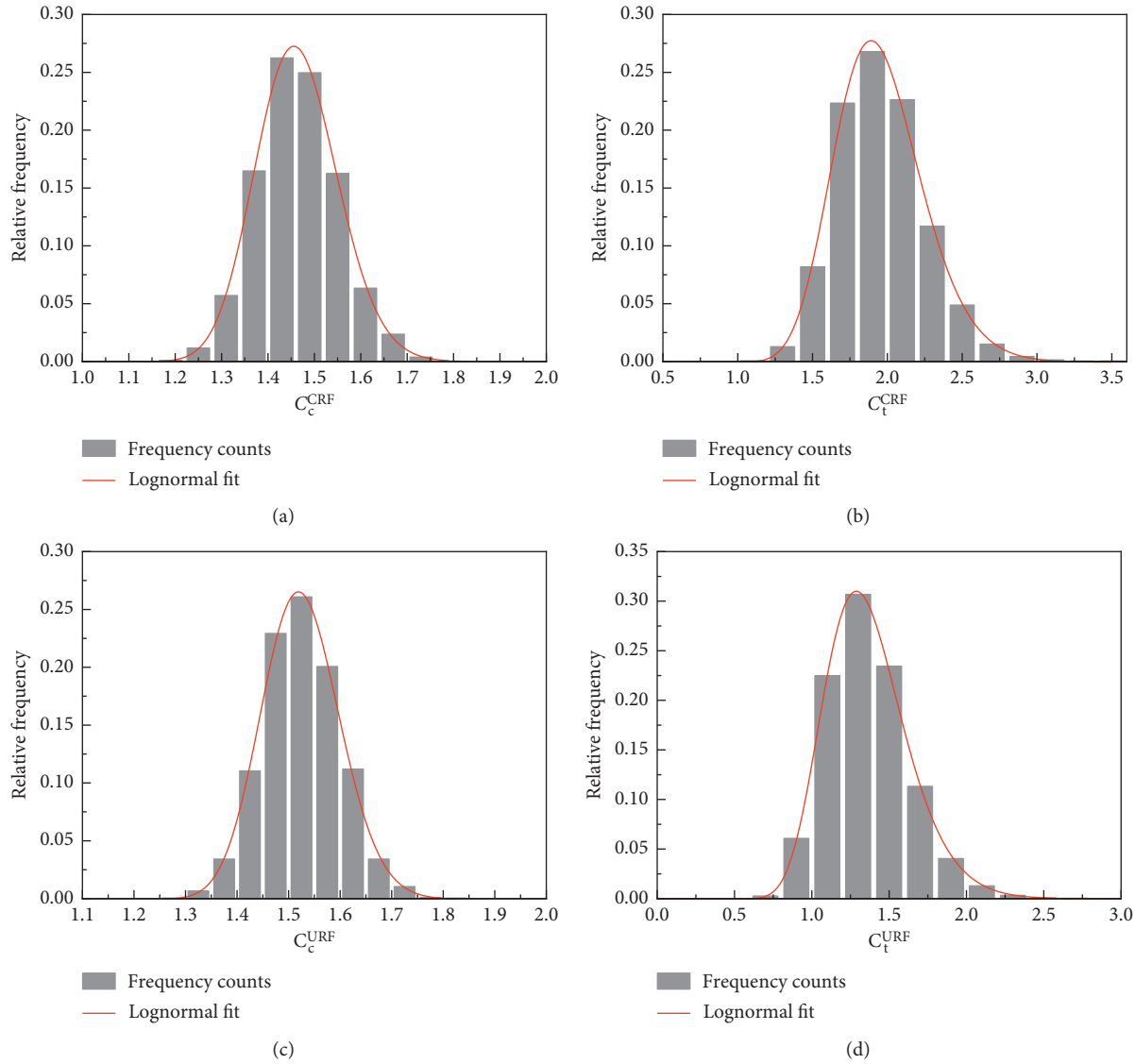

Figure 5: Typical histograms and lognormal fits of strength factors: (a) C_c^{CRF}, (b) C_t^{CRF}, (c) C_c^{URF}, and (d) C_t^{URF}.

6.4. Effect of the Vertical Correlation Length. Compared with the horizontal correlation length, the vertical correlation length has much more obvious influence on the probability of compression failure of tunnel liner, as shown in Figure 8(a). Specifically, the failure probability based on the CRF gradually decreases as the vertical correlation length increases. By contrast, the failure probability based on the URF shows a slight upward trend as the vertical correlation length rises. It should also be noted that the probability of compression failure based on the CRF is higher than that based on the URF initially and then becomes lower and lower as the vertical correlation length increases.

As for the influence on the probability of tension failure, the vertical correlation length shows some similarities with the horizontal correlation length when comparing Figure 8(b) with Figure 7(b), except that the failure probabilities based on the CRF in Figure 8(b) show a moderate upward trend instead of a downward trend.

6.5. Effect of the Cross-Correlation Coefficient. It can be seen from Figures 9(a) and 9(b) that the cross-correlation coefficient has a very significant influence on the performance of tunnel liner. To be specific, the probability of compression (tension) failure increases under both the CRF and the URF, and that increase is most clearly observed when the cross-correlation coefficient is less than 0. In addition, the probability of compression failure decreases remarkably after conditioning, as indicated in Figure 9(a). By contrast, the effect of conditioning leads to a significant increase in the probability of tension failure, as shown in Figure 9(b).

7. Reliability-Based Design of a Real Tunnel

7.1. Project Background. In this part, we conduct a reliability-based design of the tunnel liner at the cross-section level, with respect to the shield-driven tunnel section between Caihuying and Xitieying of Beijing subway line 14 (i.e., Figure 10(a)). The tunnel has a circular cross section

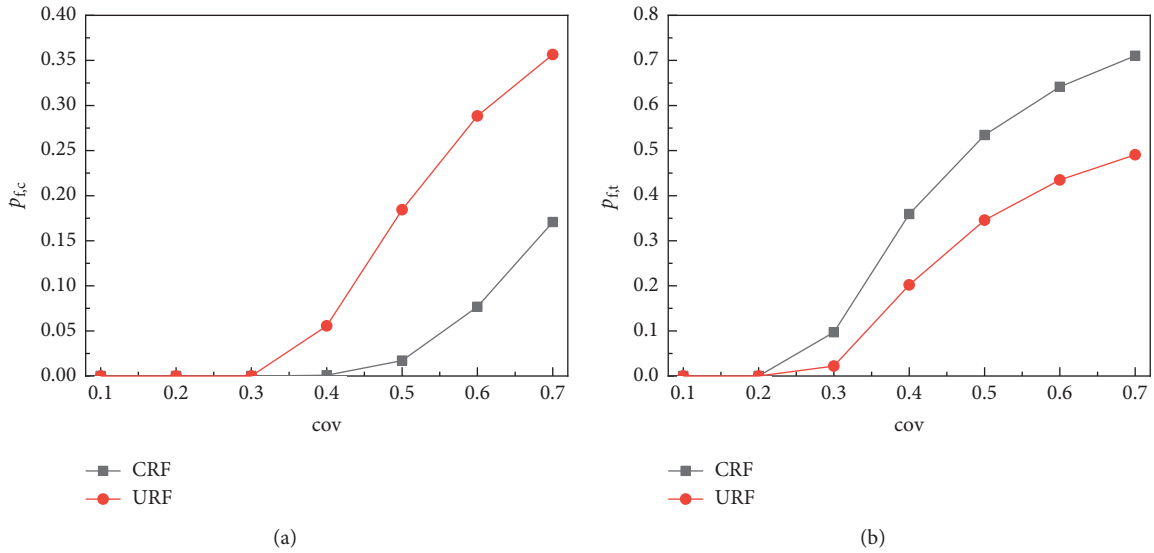

FIGURE 6: Effect of the coefficient of variation on the probability of failure of tunnel liner under both unconditional and conditional random fields: (a) compression failure and (b) tension failure.

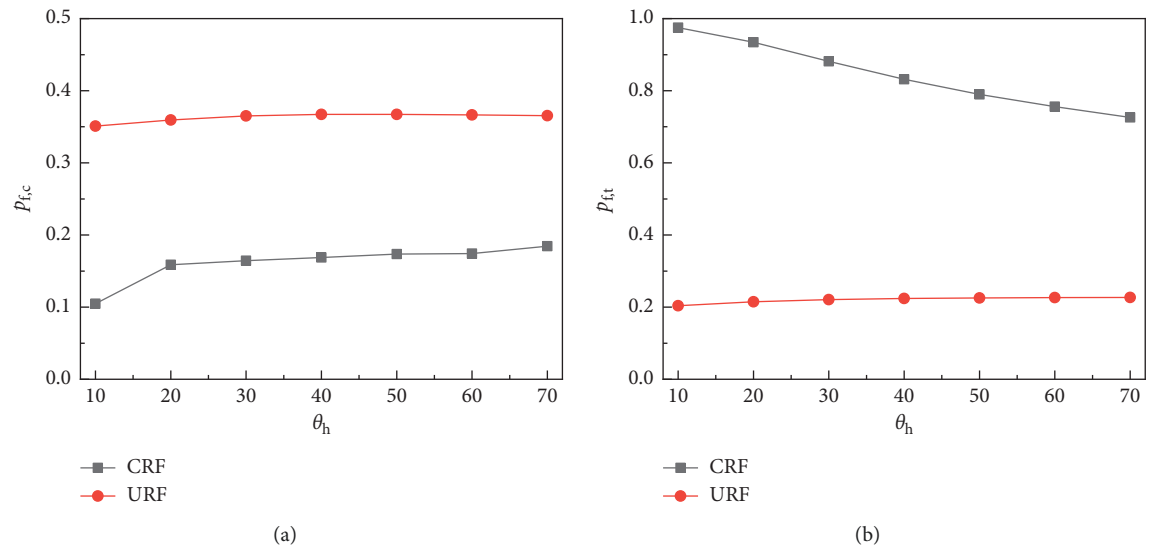

FIGURE 7: Effect of the horizontal correlation length on the probability of failure of tunnel liner under both unconditional and conditional random fields: (a) compression failure and (b) tension failure.

with a radius of 3 m and is supported by precast concrete liner, as shown in Figure 10(b). The whole length of the tunnel section is 1367.6 m, and the tunnel is driven 15.5 m to 30.7 m below the ground surface. The main soil layer through which the tunnel passes is silty clay. A total of 37 borehole logs provide the statistical information of the cohesion and friction angle of soil mass, as listed in Table 3.

Because of the limited number of borehole logs, the autocorrelation function is assumed to be equation (11), while the horizontal and vertical correlation lengths are taken to be 20 m and 5 m, respectively, in terms of the studies by Phoon and Kulhawy [61]. In addition, the cross-correlation coefficient is determined to be −0.5 with reference to Li and Low [62]. The rest soil and tunnel liner properties are considered as deterministic and used with their respective mean values, as tabulated in Table 4.

Since the procedures for evaluating the performance of the real tunnel liner are similar to those described in the previous section with respect to the hypothesized example tunnel, the major focus of this section is to conduct a reliability-based design of the real tunnel liner for practical application. Therefore, the process of conducting the probabilistic evaluation of the real tunnel liner by finite-difference modeling within the Monte Carlo simulation framework is omitted here for simplicity and only the reliability-based design is presented in the following text.

It is found that 5000 Monte Carlo simulations can also deliver comparable precision and reproducible results this

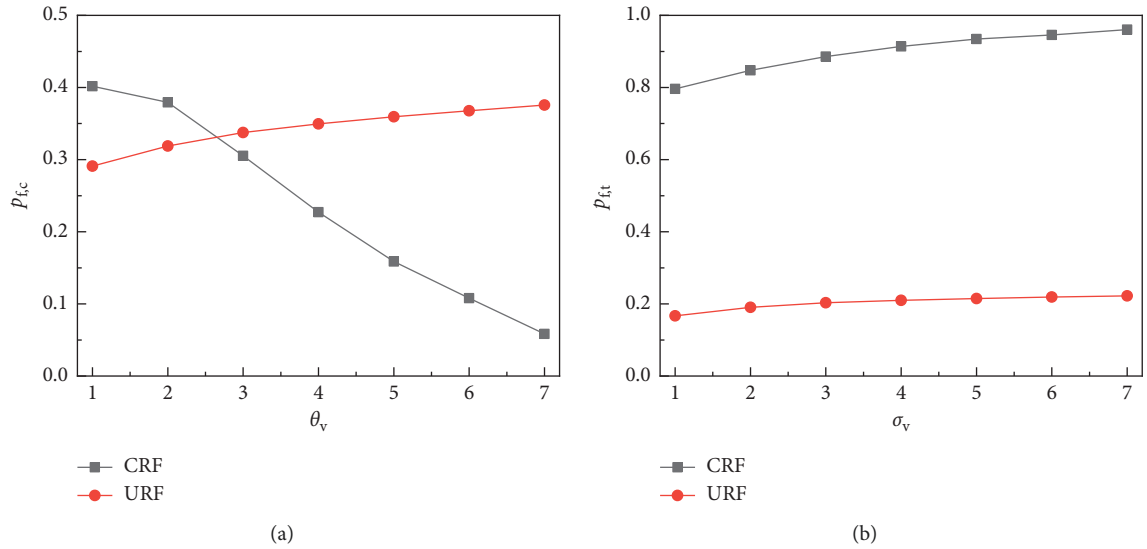

Figure 8: Effect of the vertical correlation length on the probability of failure of tunnel liner under both unconditional and conditional random fields: (a) compression failure and (b) tension failure.

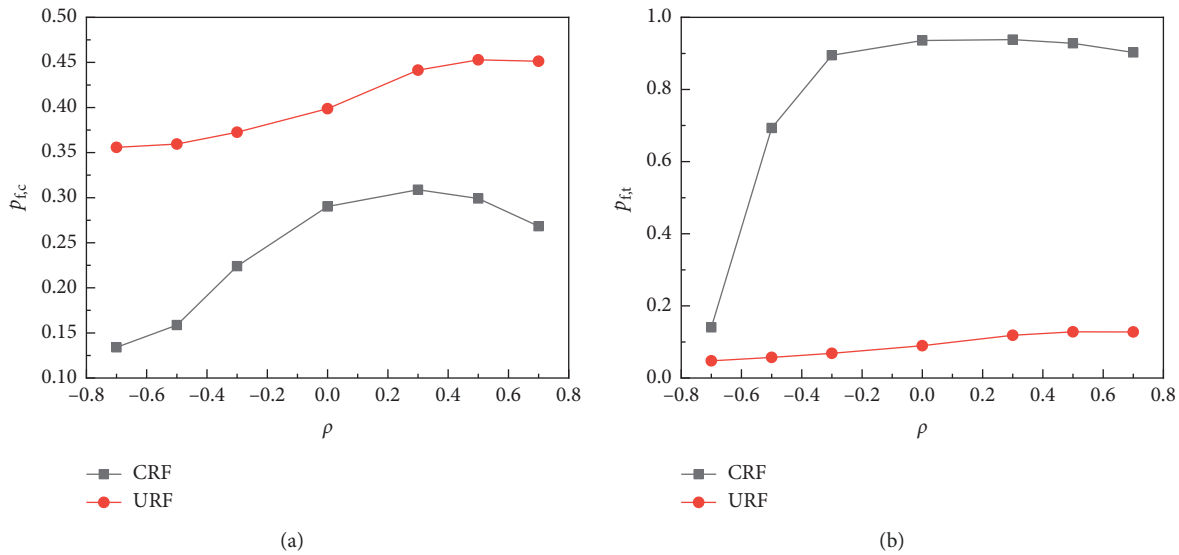

Figure 9: Effect of the cross-correlation coefficient on the probability of failure of tunnel liner under both unconditional and conditional random fields: (a) compression failure and (b) tension failure.

Figure 10: Beijing subway line 14: (a) the shield-driven tunnel entrance and (b) the precast concrete liner.

Table 3: Statistical information of the cohesion and friction angle of soil.

Property	Distribution	Max	Min	Mean	cov
Cohesion c (kPa)	Lognormal	37	13	22	0.2
Friction angle ϕ (°)		27	12	18	0.18

Table 4: Deterministic properties for the real tunnel.

Category	Property	Value
Soil	Young's modulus E_{soil} (MPa)	13
	Poisson's ratio ν_{soil}	0.2
Liner	Young's modulus E_{liner} (MPa)	30
	Poisson's ratio ν_{liner}	0.25
	Compressive strength σ_c^{liner} (MPa)	23.4
	Tensile strength σ_t^{liner} (MPa)	−2.2
	Thickness t (mm)	300

time for the real tunnel problem. So, 5000 trials are selected in the probabilistic evaluation procedure. Note that the coefficient of variation cov = 0.2 in Table 3 is used for simplicity for both cohesion and friction angle in the following reliability-based design, although the coefficient of variation of friction angle is 0.18.

7.2. Design with respect to the Compressive Strength of the Liner. A reasonable criticism of the traditional factor of safety is that it is not able to give as much physical insight into the likelihood of design failure of structures as a probabilistic measure [63]. In this subsection, a reliability-based design of the tunnel liner, with respect to liner strength, is performed by relating the conventional factor of safety to the probability of design failure for different horizontal and vertical correlation lengths, respectively, in terms of the failure modes defined in Section 4.

It would be of interest to investigate the probability of design failure of tunnel liner with respect to its compressive and tensile strengths. For instance, if the probability of failure of 0.01% is desired, then we concern about how much compressive and tensile strengths should be applied to the tunnel liner in order to meet that desired reliability.

According to the expected performance level of civil structures defined by US Army Corps of Engineers [57], we selected a set of target failure probabilities of liner in the following study, ranging from 0.1% to 0.003%, which correspond to the performance levels of "above average" to "good" [64].

For the CRF, it can be seen from Figure 11(a) that the probability of compression failure of tunnel liner rises initially and then falls gradually as the horizontal correlation length increases, for all the factors of safety. As for the URF, the failure probability increases rapidly at first, and then levels off as the horizontal correlation length rises, as indicated in Figure 11(b).

For a target failure probability $p_{f,c} = 1E-4$, the required factor of safety is $F_s = 1.82$ for the case of CRF if the horizontal correlation length is $\theta_h = 20$, which means that the concrete liner installed should at least have a compressive strength of $1.82\sigma_c^{det}$ (i.e., 27.3 MPa) in order to reach that target reliability. Note that the deterministic compressive strength of the real tunnel liner obtained from the finite-difference analysis is $\sigma_c^{det} = 15$ MPa, while a factor of safety more than $F_s = 1.82$ is required for the case of URF under the same conditions. Similar observations can also be made for other target probabilities of failure.

As can be seen from Figure 12(a) and 12(b), similar trends to what is shown in the corresponding figures of Figure 11 can be found, except that the range of change of failure probability in Figure 12 is larger than that in Figure 11. It should also be noted that the required factor of safety, given a target probability of failure, for the CRF is slightly smaller than that for the URF. For example, the required factor of safety is about $F_s = 1.82$ for the CRF if the vertical correlation length is $\theta_v = 5$ for a given target failure probability of $p_{f,c} = 1E-4$, while, for the URF, the required factor of safety is larger than $F_s = 1.82$ to reach that target reliability level, given the vertical correlation length of $\theta_v = 5$.

It should be noted that the thickness of the liner is fixed at $t = 200$ mm in the design process with respect to the compressive strength of the liner.

7.3. Design with respect to the Tensile Strength of the Liner. Figure 13(a) shows that the probability of tension failure of tunnel liner decreases as the horizontal correlation length rises. However, quite the opposite is observed in Figure 13(b) that the failure probability displays a slight upward trend as the horizontal correlation length increases. It might also be interesting to note that the required tensile strength of the liner, given a target probability of failure, for the CRF is always greater than that for the URF, as indicated in Figures 13(a) and 13(b). For example, if the target probability of failure is $p_{f,t} = 1E-4$, the liner installed should have a tensile strength of $3.4\sigma_t^{det}$ or so (i.e., −2.72 MPa) for the CRF and about $2.7\sigma_t^{det}$ (i.e., −2.16 MPa) for the URF when the horizontal correlation length is $\theta_h = 20$. Note that the deterministic tensile strength of the real tunnel liner obtained from the finite-difference analysis is $\sigma_t^{det} = -0.8$ MPa.

It can be seen from Figures 14(a) and 14(b) that similar trends to what is shown in the corresponding figures of Figure 13 can be found, except that the range of change of failure probability in Figure 14 is larger than that in Figure 13. It should also be noted that the required factor of safety, given a target probability of failure, for the CRF is always greater than that for the URF. For example, the required factor of safety is less than $F_s = 3.4$ for the CRF if the vertical correlation length is $\theta_v = 5$ for a given target failure probability of $p_{f,t} = 1E-4$, while, for the URF, the required factor of safety is about $F_s = 2.7$ to reach the target failure probability of $p_{f,t} = 1E-4$ under the vertical correlation length of $\theta_v = 5$.

It should be noted that the thickness of the liner is fixed at $t = 200$ mm in the design process with respect to the tensile strength of the liner.

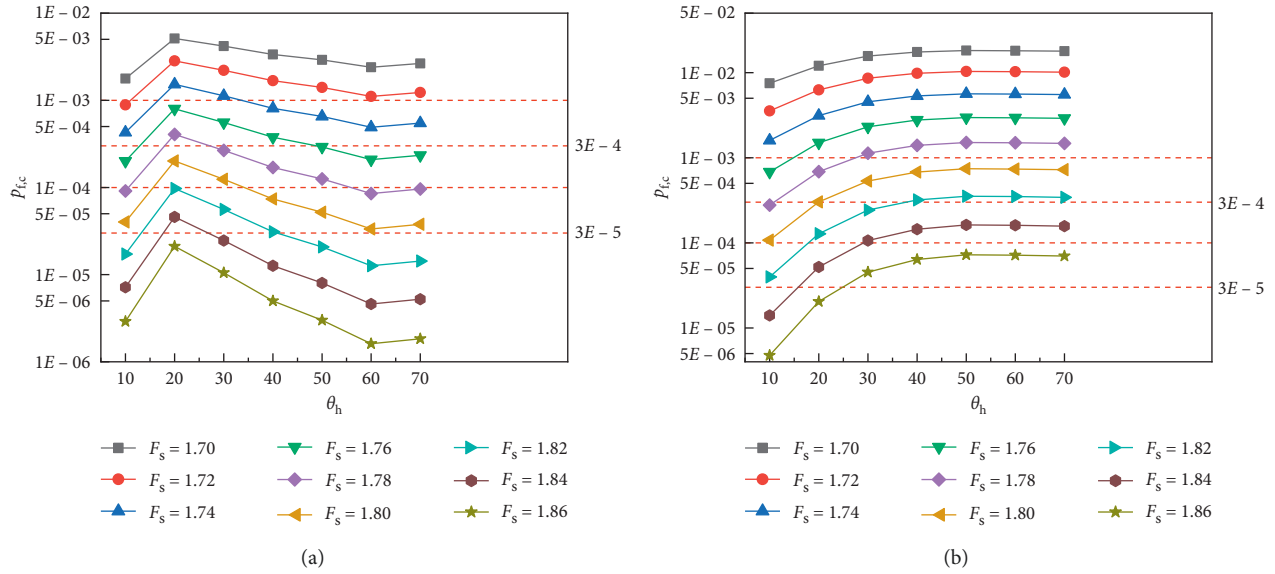

Figure 11: Probability of compression failure of tunnel liner under different random fields as a function of the horizontal correlation length and factor of safety: (a) CRF and (b) URF.

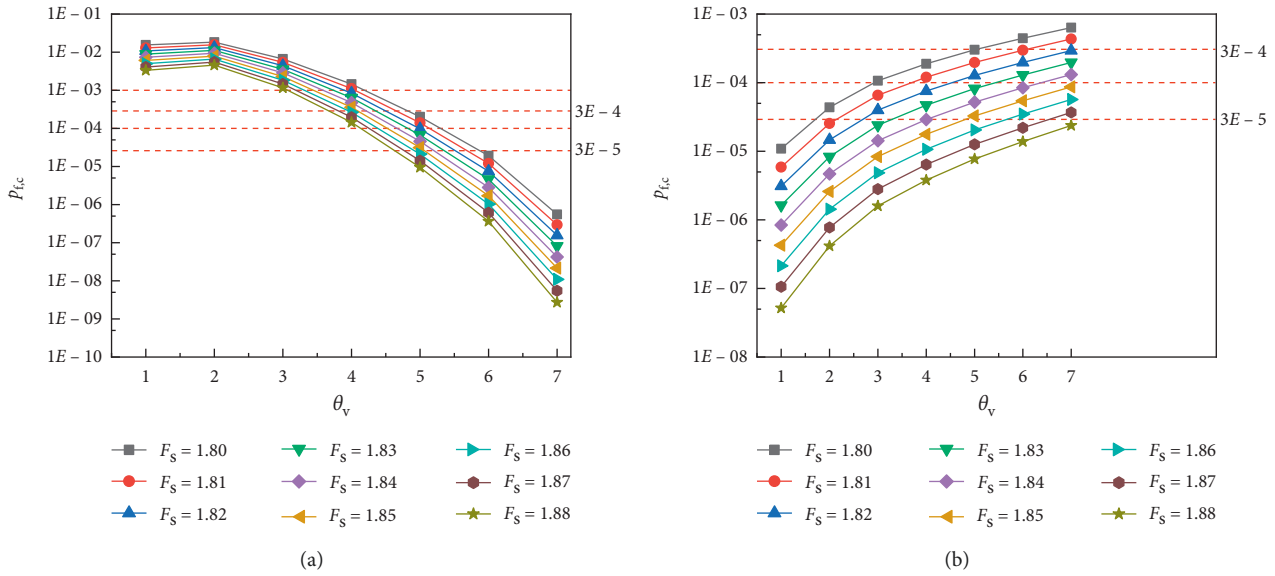

Figure 12: Probability of compression failure of tunnel liner under different random fields as a function of the vertical correlation length and factor of safety: (a) CRF and (b) URF.

7.4. Design with respect to Liner Thickness. In the case where the required liner strengths for a given target probability of failure is larger than the strength capacity of the liner installed, the thickness of the liner should be designed as an alternative method. For instance, the compressive strength designed based on the CRF in the previous subsection for the target reliability level of 0.01%, given the horizontal correlation length of $\theta_h = 20$, the vertical correlation length of $\theta_v = 5$, and the coefficient of variation of cov = 0.2, is 27.3 MPa, which is greater than the compressive strength capacity of the liner of 23.4 MPa, as listed in Table 4. In such a case, the thickness of the liner should be designed in order to meet the target reliability level of 0.01%.

In Figures 15(a) and 15(b), a relationship between the designed compressive strength (i.e., $\sigma_{c,d}^{CRF}$ and $\sigma_{c,d}^{URF}$) and liner thickness is developed based on the CRF and the URF, respectively, for four given target probabilities of failure (i.e., p_f^t = 0.1%, 0.03%, 0.01%, and 0.003%, respectively). It can be seen that the required compressive strength of liner decreases as the liner thickness is increased. When the liner thickness is increased to t = 250 mm or so, the target

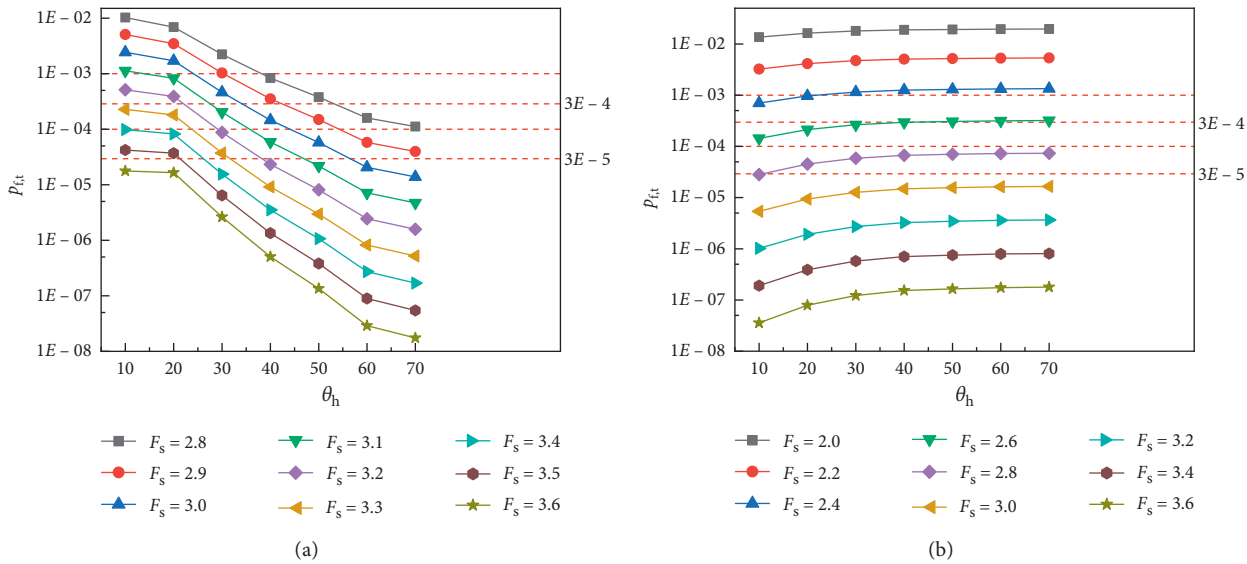

FIGURE 13: Probability of tension failure of tunnel liner under different random fields as a function of the horizontal correlation length and factor of safety: (a) CRF and (b) URF.

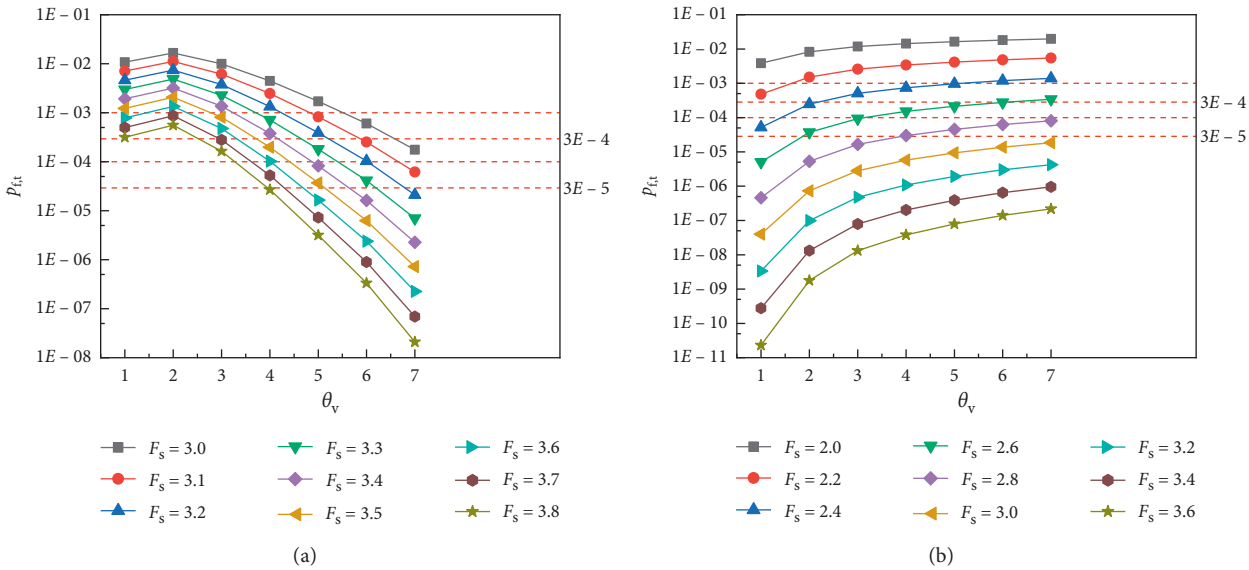

FIGURE 14: Probability of tension failure of tunnel liner under different random fields as a function of the vertical correlation length and factor of safety: (a) CRF and (b) URF.

probability of failure of 0.01% can be reached under the CRF and a liner thickness of a little more than $t = 250$ mm is required under the URF with the liner installed in this project. However, the concrete liner installed at the real tunnel has a thickness of $t = 300$ mm, as indicated in Figure 16. It can be, therefore, argued that the precast concrete liner installed at the tunnel project is too conservative.

It can be seen from Figures 17(a) and 17(b) that the absolute value of the desired tensile strength (i.e., $\sigma_{t,d}^{CRF}$ and $\sigma_{t,d}^{URF}$) decreases as the liner becomes increasingly thick under both the CRF and the URF. However, the target reliability level can be reached, given a specific liner thickness is very different for the CRF and URF. For example, the highest performance level under the CRF can be reached for the liner installed in this project is about $p_f^t = 0.01\%$ if the liner has a thickness of $t = 250$ mm, while a target probability of failure of far less than $p_f^t = 0.003\%$ can be achieved under the URF.

No matter the performance of tunnel liner evaluated based on the CRF or the URF, the precast concrete liner installed at the tunnel project, which has a thickness of $t = 300$ mm, is thick enough to reach the target reliability level of $p_f^t = 0.01\%$, which means that the liner thickness is too conservative and should be much thinner from the perspective of reliability-based design.

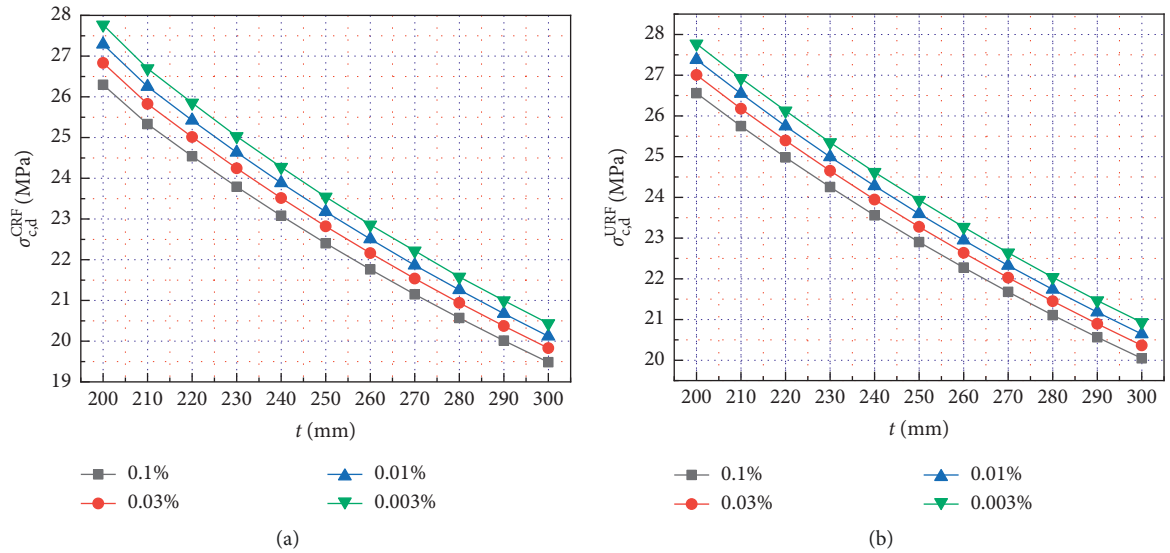

Figure 15: The relationship between the designed compressive strength and liner thickness under different random fields for different target probabilities of failure: (a) CRF and (b) URF.

Figure 16: A realistic photo indicating the thickness of the precast concrete liner.

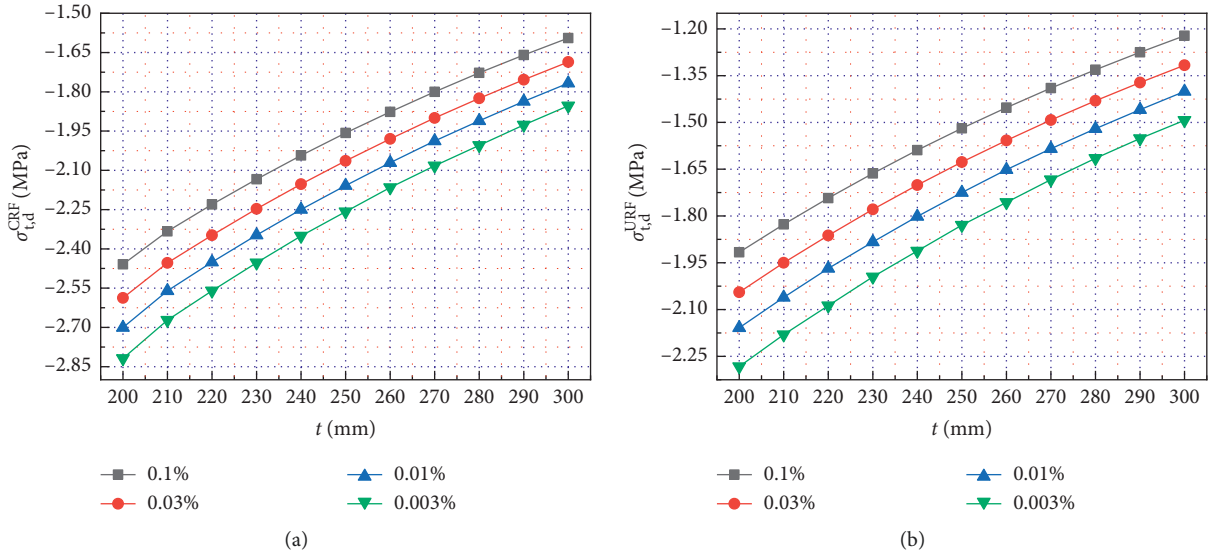

Figure 17: The relationship between the designed tensile strength and liner thickness under different random fields for different target probabilities of failure: (a) CRF and (b) URF.

8. Summary and Conclusions

Although it is widely recognized that the soil properties are spatially variable and a sufficient amount of borehole drillings are usually carried out before tunnel excavation, this has not led to a widespread application of random field methods, especially conditional random field method, to the design of tunnel supports (e.g., tunnel liner). However, the probabilistic evaluation and design of tunnel support based on random fields can result in a better understanding of the relationship between the tunnel risk and the required target reliability level, which in turn leads to more reasonable and cost-effective decision-making on the selection of appropriate support type and support parameters.

In this paper, a probabilistic procedure for evaluating the tunnel liner performance is clearly described first and then applied to a hypothesized tunnel to investigate the effects of site characterization parameters and conditioning on the tunnel liner performance. In addition, a reliability-based design of a real tunnel at Beijing subway line 14 is conducted using the probabilistic evaluation procedure described above, in which the borehole logs at the project site are fully taken account of and the measured data values are applied in the construction of the conditional random field. According to the results from the parametric studies and the reliability-based design, we find that the conditioning and site characterization parameters, including the coefficient of variation, the horizontal (vertical) correlation length, and the cross-correlation coefficient all have significant effects on the performance of tunnel liner. Specifically, a number of conclusions can be drawn as follows:

(1) For failures in compression and tension, the failure probability increases obviously as the coefficient of variation rises, especially for the medium to high values of coefficient of variation (e.g., cov = 0.3 to cov = 0.7). However, the tunnel liner is less likely to fail in compression and more prone to fail in tension after conditioning the random field on the measured data obtained at the borehole locations.

(2) The probabilities based on the URF are almost unchanged as the horizontal correlation length varies for both failures in compression and in tension. However, the probabilities based on the CRF show a slight upward trend for failure in compression and a downward trend for failure in tension.

(3) The vertical correlation length has very similar but more obvious effects on both failures in compression and in tension compared with the horizontal correlation length, especially for the compression failure based on the CRF.

(4) For failures in compression and tension, the probabilities based on the CRF are much more affected by the variation of the cross-correlation coefficient, especially when the cross-correlation coefficient is less than 0, while the probabilities based on the URF are less influenced by the cross-correlation efficient, especially for the probabilities of tension failure.

(5) The effect of conditioning on the performance of liner is very significant. For all the site characterization parameters included in the parametric study, the probability decreases for failure in compression and increases for failure in tension after conditioning. That is to say the measured data at the borehole locations should be considered in the probabilistic evaluation procedure and the effect of conditioning should be honored.

(6) The probabilistic evaluation procedure can relate the probability of design failure with the more conventional factor of safety, which facilitates the reliability-based design of the tunnel liner in practice by directly applying the corresponding factor of safety to the target reliability level. Besides, it is also capable of associating the liner strength capacity with the liner thickness for a given target reliability level, which implies that the probabilistic evaluation procedure allows flexibility in application.

(7) The probabilistic evaluation procedure described in this study can lead to more reasonable and economical designs of tunnel liner in practice, given the required reliability level.

The motivation of this study is to provide some general insights into the area of reliability analysis and design of tunnel liner with consideration of conditional random field theory combined with finite-difference modeling using FLAC 3D in the framework of Monte Carlo simulation. The present work is also motivated by the desire to offer tunnel engineers with a general procedure for conducting reliability-based analysis and design of tunnel liner in practice.

With these motivations in mind, the investigation in this paper is carried out and the conclusions drawn above can provide tunnel engineers with evidence that site-specific investigation should not be ignored and the randomness and spatial variability of soil properties should be seriously considered in the design of tunnel support; especially, the measured data values from the borehole logs should be honored.

Although the reliability-based design of the tunnel liner in this study is performed with consideration of the measured data values from the borehole logs, some problems still exist. Due to the limited number of borehole logs and the amount of computation effort required, the present work is conducted with the assumptions of (1) stationary random field with constant mean and variance throughout the domain; (2) exponential autocorrelation structure with the horizontal and vertical correlation lengths of 20 m and 5 m, respectively; (3) cross-correlation coefficient of −0.5 between cohesion and friction angle; and (4) 2-dimensional finite-difference model at the cross-section level. Therefore, care should be taken for interested readers when dealing with real projects where geological and geotechnical conditions may be different or much more complicated.

Data Availability

The data used to support the findings of this study are included in the article.

Conflicts of Interest

The authors declare that there are no conflicts of interest regarding the publication of this paper.

Acknowledgments

The financial support from the National Key R&D Program of China (no. 2016YFC0600901), the State Key Laboratory for Geomechanics and Deep Underground Engineering, and the Natural Science Foundation of China (nos. 41172116 and U1261212) is all gratefully acknowledged.

References

[1] C. Carranza-Torres and M. Diederichs, "Mechanical analysis of circular liners with particular reference to composite supports. For example, liners consisting of shotcrete and steel sets," *Tunnelling and Underground Space Technology*, vol. 24, no. 5, pp. 506–532, 2009.

[2] O. Arnau and C. Molins, "Experimental and analytical study of the structural response of segmental tunnel linings based on an in situ loading test. Part 2: numerical simulation," *Tunnelling and Underground Space Technology*, vol. 26, no. 6, pp. 778–788, 2011.

[3] J. C. Langford and M. S. Diederichs, "Reliability-based approach to tunnel lining design using a modified point estimate method," *International Journal of Rock Mechanics and Mining Sciences*, vol. 60, pp. 263–276, 2013.

[4] N. A. Do, D. Dias, P. Oreste, and D.-M. Irini, "The behaviour of the segmental tunnel lining studied by the hyperstatic reaction method," *European Journal of Environmental and Civil Engineering*, vol. 18, no. 4, pp. 489–510, 2014.

[5] H.-W. Huang and D.-M. Zhang, "Resilience analysis of shield tunnel lining under extreme surcharge: characterization and field application," *Tunnelling and Underground Space Technology*, vol. 51, pp. 301–312, 2016.

[6] C. Zhao, A. Alimardani Lavasan, T. Barciaga, C. Kämper, P. Mark, and T. Schanz, "Prediction of tunnel lining forces and deformations using analytical and numerical solutions," *Tunnelling and Underground Space Technology*, vol. 64, pp. 164–176, 2017.

[7] H. M. Kroetz, N. A. Do, D. Dias, and A. T. Beck, "Reliability of tunnel lining design using the hyperstatic reaction method," *Tunnelling and Underground Space Technology*, vol. 77, pp. 59–67, 2018.

[8] N.-A. Do and D. Dias, "Tunnel lining design in multi-layered grounds," *Tunnelling and Underground Space Technology*, vol. 81, pp. 103–111, 2018.

[9] Y. Jiang, X. Zhang, and T. Taniguchi, "Quantitative condition inspection and assessment of tunnel lining," *Automation in Construction*, vol. 102, pp. 258–269, 2019.

[10] W. Song, H. Lai, Y. Liu, W. Yang, and Z. Zhu, "Field and laboratory study of cracking and safety of secondary lining for an existing highway tunnel in loess ground," *Tunnelling and Underground Space Technology*, vol. 88, pp. 35–46, 2019.

[11] D. V. Griffiths and G. A. Fenton, "Seepage beneath water retaining structures founded on spatially random soil," *Géotechnique*, vol. 43, no. 4, pp. 577–587, 1993.

[12] D. V. Griffiths and G. A. Fenton, "Probabilistic slope stability analysis by finite elements," *Journal of Geotechnical and Geoenvironmental Engineering*, vol. 130, no. 5, pp. 507–518, 2004.

[13] G. A. Fenton and D. V. Griffiths, "Bearing-capacity prediction of spatially random c—ϕ soils," *Canadian Geotechnical Journal*, vol. 40, no. 1, pp. 54–65, 2003.

[14] S. H. Jiang, D. Q. Li, Z. J. Cao, C.-B. Zhou, and V Phoon, "Efficient system reliability analysis of slope stability in spatially variable soils using Monte Carlo simulation," *Journal of Geotechnical and Geoenvironmental Engineering*, vol. 141, no. 2, Article ID 04014096, 2014.

[15] D.-Q. Li, S.-H. Jiang, Z.-J. Cao, W. Zhou, C.-B. Zhou, and L.-M. Zhang, "A multiple response-surface method for slope reliability analysis considering spatial variability of soil properties," *Engineering Geology*, vol. 187, pp. 60–72, 2015.

[16] Y. Wang, Z. Cao, and D. Li, "Bayesian perspective on geotechnical variability and site characterization," *Engineering Geology*, vol. 203, pp. 117–125, 2016.

[17] E. H. Vanmarcke, *Random Fields: Analysis and Synthesis*, MIT Press, Cambridge, MA, USA, 1983.

[18] D. V. Griffiths, J. Huang, and G. A. Fenton, "Probabilistic slope stability analysis using RFEM with non-stationary random fields," in *Geotechnical Safety*, V. Risk, T. Schweckendiek, A. F. van Tol, and D. Pereboom, Eds., pp. 704–709, 2015.

[19] S.-H. Jiang, J. Huang, and C.-B. Zhou, "Efficient system reliability analysis of rock slopes based on subset simulation," *Computers and Geotechnics*, vol. 82, pp. 31–42, 2017.

[20] S.-H. Jiang and J. Huang, "Modeling of non-stationary random field of undrained shear strength of soil for slope reliability analysis," *Soils and Foundations*, vol. 58, no. 1, pp. 185–198, 2018.

[21] Q. Chen, A. Seifried, J. E. Andrade, and J. W. Baker, "Characterization of random fields and their impact on the mechanics of geosystems at multiple scales," *International Journal for Numerical and Analytical Methods in Geomechanics*, vol. 36, no. 2, pp. 140–165, 2012.

[22] Y. J. Li, M. A. Hicks, and P. J. Vardon, "Uncertainty reduction and sampling efficiency in slope designs using 3D conditional random fields," *Computers and Geotechnics*, vol. 79, pp. 159–172, 2016.

[23] G. Mollon, D. Dias, and A.-H. Soubra, "Probabilistic analysis of circular tunnels in homogeneous soil using response surface methodology," *Journal of Geotechnical and Geoenvironmental Engineering*, vol. 135, no. 9, pp. 1314–1325, 2009.

[24] G. Mollon, D. Dias, and A.-H. Soubra, "Probabilistic analysis and design of circular tunnels against face stability," *International Journal of Geomechanics*, vol. 9, no. 6, pp. 237–249, 2009.

[25] K.-I. Song, G.-C. Cho, and S.-W. Lee, "Effects of spatially variable weathered rock properties on tunnel behavior," *Probabilistic Engineering Mechanics*, vol. 26, no. 3, pp. 413–426, 2011.

[26] N.-A. Do, D. Dias, P. Oreste, and I. Djeran-Maigre, "2D numerical investigation of segmental tunnel lining behavior," *Tunnelling and Underground Space Technology*, vol. 37, pp. 115–127, 2013.

[27] D. K. E. Green, K. Douglas, and G. Mostyn, "The simulation and discretisation of random fields for probabilistic finite element analysis of soils using meshes of arbitrary triangular

elements," *Computers and Geotechnics*, vol. 68, pp. 91–108, 2015.

[28] M. E. Daryani, H. Bahadori, and K. E. Daryani, "Soil probabilistic slope stability analysis using stochastic finite difference method," *Modern Applied Science*, vol. 11, no. 4, p. 23, 2017.

[29] Q. Lü, Z. P. Xiao, J. Zheng, and Y. Shang, "Probabilistic assessment of tunnel convergence considering spatial variability in rock mass properties using interpolated autocorrelation and response surface method," *Geoscience Frontiers*, vol. 9, no. 6, pp. 1619–1629, 2017.

[30] R. Acharyya and A. Dey, "Finite element investigation of the bearing capacity of square footings resting on sloping ground," *INAE Letters*, vol. 2, no. 3, pp. 97–105, 2017.

[31] A. P. Dyson and A. Tolooiyan, "Prediction and classification for finite element slope stability analysis by random field comparison," *Computers and Geotechnics*, vol. 109, pp. 117–129, 2019.

[32] J. W. Cooley and J. W. Tukey, "An algorithm for the machine calculation of complex Fourier series," *Mathematics of Computation*, vol. 19, no. 90, p. 297, 1965.

[33] G. Matheron, "The intrinsic random functions and their applications," *Advances in Applied Probability*, vol. 5, no. 03, pp. 439–468, 1973.

[34] A. Der Kiureghian and J.-B. Ke, "The stochastic finite element method in structural reliability," *Probabilistic Engineering Mechanics*, vol. 3, no. 2, pp. 83–91, 1988.

[35] G. A. Fenton and E. H. Vanmarcke, "Simulation of random fields via local average subdivision," *Journal of Engineering Mechanics*, vol. 116, no. 8, pp. 1733–1749, 1990.

[36] K. K. Phoon, S. P. Huang, and S. T. Quek, "Implementation of Karhunen-Loeve expansion for simulation using a wavelet-galerkin scheme," *Probabilistic Engineering Mechanics*, vol. 17, no. 3, pp. 293–303, 2002.

[37] G. A. Fenton and D. V. Griffiths, *Risk Assessment in Geotechnical Engineering*, John Wiley & Sons, Hoboken, NJ, USA, 2008.

[38] Y. Hoffman and E. Ribak, "Constrained realizations of Gaussian fields—a simple algorithm," *The Astrophysical Journal*, vol. 380, pp. L5–L8, 1991.

[39] Y. Hoffman, "Gaussian fields and constrained simulations of the large-scale structure," in *Data Analysis in Cosmology*, pp. 565–583, Springer, Berlin, Heidelberg, Germany, 2008.

[40] R. Schöbi and B. Sudret, "Application of conditional random fields and sparse polynomial chaos expansions to geotechnical problems," *Geotechnical Safety and Risk*, vol. 445, 2015.

[41] R. Schöbi and B. Sudret, "Application of conditional random fields and sparse polynomial chaos expansions in structural reliability analysis," in *Proceedings of the 12th International Conference on Structural Safety and Reliability*, pp. 1356–1363, Vienna, Austria, August 2017.

[42] W. Gong, C. H. Juang, J. R. Martin, H. Tang, Q. Wang, and H. Huang, "Probabilistic analysis of tunnel longitudinal performance based upon conditional random field simulation of soil properties," *Tunnelling and Underground Space Technology*, vol. 73, pp. 1–14, 2018.

[43] X. Y. Li, L. M. Zhang, and J. H. Li, "Using conditioned random field to characterize the variability of geologic profiles," *Journal of Geotechnical and Geoenvironmental Engineering*, vol. 142, no. 4, Article ID 04015096, 2016.

[44] M. Lloret-Cabot, M. A. Hicks, and A. P. Van Den Eijnden, "Investigation of the reduction in uncertainty due to soil variability when conditioning a random field using Kriging," *Géotechnique Letters*, vol. 2, no. 3, pp. 123–127, 2012.

[45] L.-L. Liu, Y.-M. Cheng, and S.-H. Zhang, "Conditional random field reliability analysis of a cohesion-frictional slope," *Computers and Geotechnics*, vol. 82, pp. 173–186, 2017.

[46] Itasca and FLAC, *Fast Lagrangian Analysis of Continua, Version 5.0*, Itasca Consulting Group, Inc., Minneapolis, MN, USA, 2005.

[47] G. Mollon, K. K. Phoon, D. Dias, and A.-H. Soubra, "Influence of the scale of fluctuation of the friction angle on the face stability of a pressurized tunnel in sands," in *Proceedings of the ASCE Georisk: Geotechnical Risk Assessment and Management*, Atlanta, Georgia, June 2011.

[48] S. Senent and R. Jimenez, "A tunnel face failure mechanism for layered ground, considering the possibility of partial collapse," *Tunnelling and Underground Space Technology*, vol. 47, pp. 182–192, 2015.

[49] H.-Z. Cheng, J. Chen, R.-P. Chen, and G.-L. Chen, "Reliability study on shield tunnel face using a random limit analysis method in multilayered soils," *Tunnelling and Underground Space Technology*, vol. 84, pp. 353–363, 2019.

[50] A. Napoli, *DMJM Harris-Arup Joint Venture, Second Ave. Subway Project*, Personal Communication, New York, NY, USA, 2007.

[51] Y. Wang, Z. Cao, and S. K. Au, "Efficient Monte Carlo simulation of parameter sensitivity in probabilistic slope stability analysis," *Computers and Geotechnics*, vol. 37, no. 7-8, pp. 1015–1022, 2010.

[52] Y. Wang, "Reliability-based design of spread foundations by Monte Carlo simulations," *Géotechnique*, vol. 61, no. 8, pp. 677–685, 2011.

[53] A. J. Li, M. J. Cassidy, Y. Wang, R. S. Merifield, and A. V. Lyamin, "Parametric Monte Carlo studies of rock slopes based on the Hoek-Brown failure criterion," *Computers and Geotechnics*, vol. 45, pp. 11–18, 2012.

[54] L. Li and X. Chu, "Locating the multiple failure surfaces for slope stability using Monte Carlo technique," *Geotechnical and Geological Engineering*, vol. 34, no. 5, pp. 1475–1486, 2016.

[55] A. Mahdiyar, M. Hasanipanah, D. J. Armaghani et al., "A Monte Carlo technique in safety assessment of slope under seismic condition," *Engineering with Computers*, vol. 33, no. 4, pp. 807–817, 2017.

[56] Z. Wu, J. Yang, T. Qiu et al., "Stochastic analysis of layered rock slope stability with Monte Carlo simulations," in *Proceedings of the ISRM International Symposium-10th Asian Rock Mechanics Symposium*, Singapore, October 2018.

[57] D. J. Kamien, *Engineering and Design: Introduction to Probability and Reliability Methods for Use in Geotechnical Engineering*, Corps Of Engineers, Washington, DC, USA, 1997.

[58] J. Zhang, H. Z. Chen, H. W. Huang, and Z. Luo, "Efficient response surface method for practical geotechnical reliability analysis," *Computers and Geotechnics*, vol. 69, pp. 496–505, 2015.

[59] H. Liu and B. K. Low, "System reliability analysis of tunnels reinforced by rockbolts," *Tunnelling and Underground Space Technology*, vol. 65, pp. 155–166, 2017.

[60] Q. Pan and D. Dias, "Probabilistic evaluation of tunnel face stability in spatially random soils using sparse polynomial chaos expansion with global sensitivity analysis," *Acta Geotechnica*, vol. 12, no. 6, pp. 1415–1429, 2017.

[61] K.-K. Phoon and F. H. Kulhawy, "Characterization of geotechnical variability," *Canadian Geotechnical Journal*, vol. 36, no. 4, pp. 612–624, 1999.

[62] H. Z. Li and B. K. Low, "Reliability analysis of circular tunnel under hydrostatic stress field," *Computers and Geotechnics*, vol. 37, no. 1-2, pp. 50–58, 2010.

[63] A. Singh, "How reliable is the factor of safety in foundation engineering," in *Proceedings of the First International Conference on Applications of Statistics and Probability to Soil and Structural Engineering*, P. Lumb, Ed., pp. 390–409, Hong Kong University Press, Hong Kong, China, February 1972.

[64] Y. Wang and F. H. Kulhawy, "Reliability index for serviceability limit state of building foundations," *Journal of Geotechnical and Geoenvironmental Engineering*, vol. 134, no. 11, pp. 1587–1594, 2008.